Chinese Journal of Catalysis 70 (2025) 444–454

available at www.sciencedirect.com

ScienceDirect

journal homepage: www.sciencedirect.com/journal/chinese-journal-of-catalysis

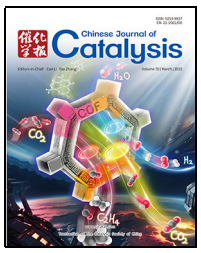

Article

Unified construction of prenylated and reverse-prenylated oxindoles from isoprene launched by Ni catalysis

Ying-Ying Liu [a,b], Ying Li [a,b], Xue-Ting Li [a,b], Su-Yang Xu [a,b], Ding-Wei Ji [a,*], Xiang-Ping Hu [a,b,*], Qing-An Chen [a,b,*]

[a] *Dalian Institute of Chemical Physics, Chinese Academy of Sciences, Dalian 116023, Liaoning, China*
[b] *University of Chinese Academy of Sciences, Beijing 100049, China*

ARTICLE INFO

Article history:
Received 3 December 2024
Accepted 20 December 2024
Available online 20 March 2025

Keywords:
Nickel catalysis
Unified construction
Isoprene
(Reverse-)prenylation
Oxindole

ABSTRACT

As important natural and pharmaceutical motifs, the catalytic construction of structurally diverse 3,3-disubstituted oxindoles often requires elaborate synthetic efforts on optimizations. Herein, we developed a simple and divergent approach for constructing reverse-prenylated and prenylated oxindoles launched by Ni catalysis with bulk chemical isoprene. Using C3-unsubstituted oxindoles as starting materials, mono reverse-prenylation was demonstrated in high chemo- and regioselectivities facilitated by the combination of Ni(0) and monodentate phosphine ligand. Using the obtained reverse-prenylated oxindoles as versatile synthon, substitutions at the pseudobenzylic position with various electrophiles created vicinal quaternary centers in a concise way. With the help of additives (PPh_3 and NaH), air could be directly used as green oxidant to construct prenylated and reverse-prenylated α-hydroxy-oxindoles divergently from the same substrates. In situ esterification of prenylated α-hydroxy-oxindoles allowed subsequent Friedel-Crafts substitutions with diverse nucleophiles to deliver prenyl substituted dimeric or spiro-oxindoles. This protocol provides a divergent synthetic approach for the construction of highly functionalized 3,3-disubstituted oxindoles, which have been otherwise difficult to access in a unified approach.

1. Introduction

The rapid assembly of privileged scaffolds from readily available starting materials is of crucial importance in the discovery of new drug candidates [1]. Oxindoles are very common structural motifs in a variety of natural alkaloids and synthetic pharmaceutical molecules [2]. Among them, the oxindole alkaloids bearing a prenyl or reverse-prenyl group at the C3 position are of particular interest due to their broad spectrum of biological activities [3]. For example, Spirotryprostatin B is isolated from fermentation of Aspergillus fumigatus with enhanced inhibitory activity over the growth of human chronic myelogenous leukemia [4]. Notoamide C exhibits significant cytotoxicity against a panel of cancer cell lines [5]. On the other hand, 3-(reverse-)prenylated oxindoles are also widely served as key building blocks for the synthesis of many indole alkaloids such as the flustramine family (Fig. 1(A)) [6,7]. Traditionally, incorporation of these desired (reverse-)prenylated groups onto oxindoles suffer from stoichiometric amounts of waste [8–12], low functional group tolerance or pre-preparation of suitable precursors [13–18]. Besides, the regioselectivity in these protocols mainly depends on the intrinsic properties of oxindole substrates or prenylic reagents, the controllable installation of prenyl and reverse prenyl units

* Corresponding author. E-mail: dingweiji@dicp.ac.cn (D.-W. Ji), xiangping@dicp.ac.cn (X.-P. Hu), qachen@dicp.ac.cn (Q.-A. Chen).
This work was supported by the National Natural Science Foundation of China (22201281, 22071239, 22371275).
https://doi.org/10.1016/S1872-2067(24)60218-4

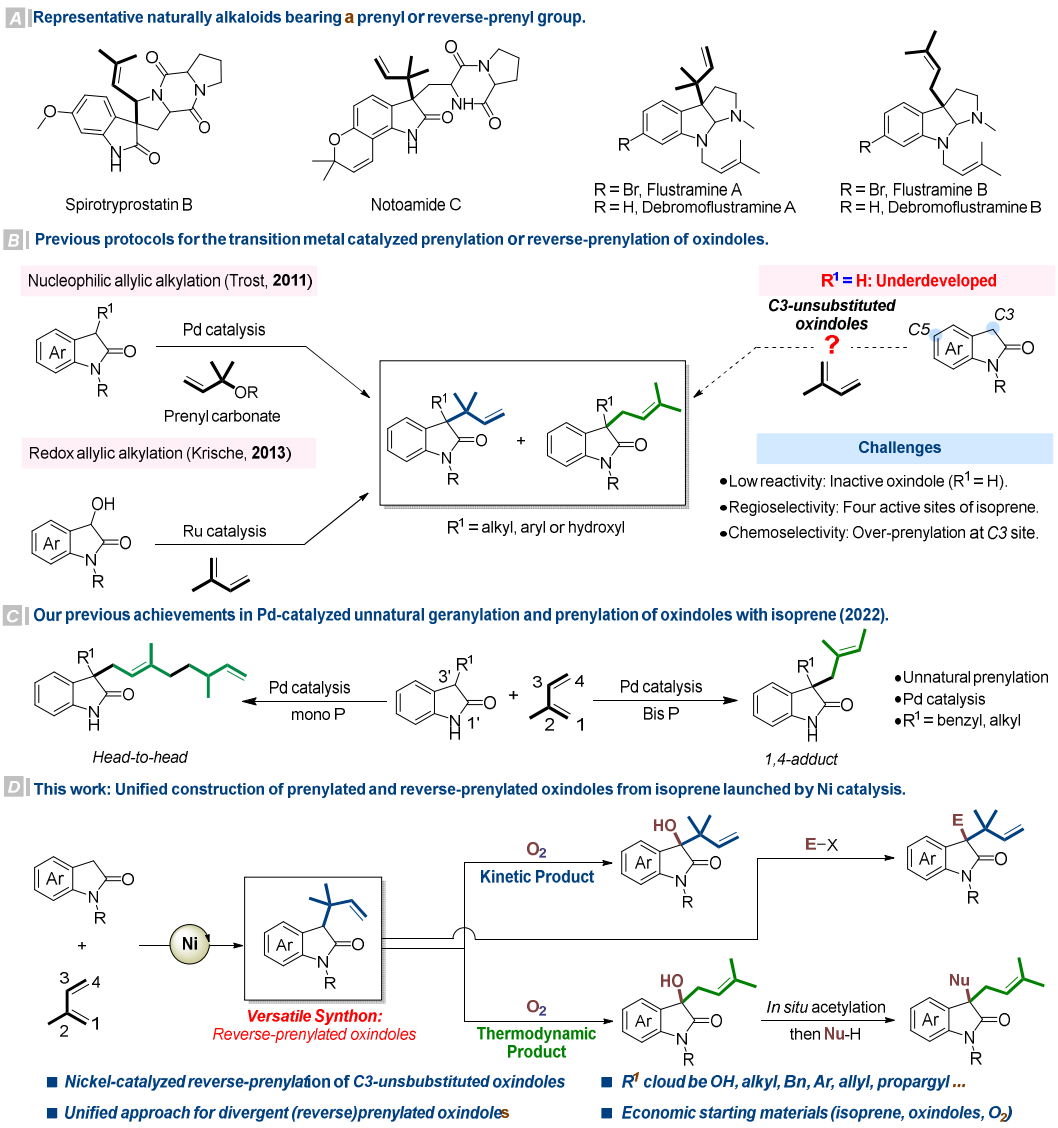

Fig. 1. Unified construction of prenylated and reverse-prenylated oxindoles from isoprene launched by Ni catalysis.

would become a formidable task in these protocols [19].

Development of transition metal-catalyzed allylic alkylation has played an irreplaceable role in allowing synthetic approach to biologically important molecules [20–24]. In 2011, a milestone for the controllable synthesis of prenylated and reverse-prenylated oxindoles was achieved by Trost and colleagues through palladium catalyzed nucleophilic allylic substitution [25]. Then Krische's group [26] also reported a redox triggered prenylation of 3-hydroxyoxindole with isoprene under ruthenium catalysis (Fig. 1(B)). Despite these advancements, it should be noticed that while C3-substituted substrates (R^1 = alkyl or OH) were especially vital to guarantee the desired reactivities or selectivities. Due to intrinsic electron and steric hindrance properties, the presence of different substitutes (R^1) will require a risk development on new catalytic system for a new target. Therefore, we wondered to develop a unified and alternative approach to allow the selective prenylation or reverse-prenylation with C3-unsubstituted oxindoles before the incorporation of different substitutes (R^1).

There are three main challenges may perplex the metal catalyzed (reverse-)prenylic alkylation of C3-unsubstituted oxindoles with isoprene: (1) The C3-substituents intended to participate in the formation of key intermediates and spatial configuration, so it would be difficult to maintain the reactivity or selectivity when such substituted groups removed; (2) Isoprene has four electrophilic sites derived from the electronically unbiased alkenyl carbon atoms, so the regioselective control may become a daunting task; (3) For the transition metal catalyzed allylic alkylation reactions, the generated C3-monosubstituted oxindole products would exhibit higher tendency to the next prenylation *via* facile enolate isomerization. As a result, the control of chemoselectivity may be an additional obstacle as well. Therefore, it calls for an urgent need of a robust catalysis to allow the selective prenylation or reverse-prenylation with C3-unsubstituted oxindoles. Based on our continuous research on hydrofunctionalization of isoprene [27–32], the ligand-regulated unnatural prenylation and geranylation of oxindoles with isoprene under Pd catalysis was

achieved in 2022 (Fig. 1(C)) [27]. To switch the regioselectivity and extend the substrate scope to more challenging C3-unsubstituted oxindoles, here we developed an efficient and atom-economic nickel catalysis for first realizing the selective reverse-prenylation of C3-unsubstituted oxindoles (Fig. 1(D)). More importantly, taking advantage of the remaining C-H bond at C3-position, we found prenylated and reverse-prenylated α-hydroxy-oxindoles could be divergently achieved by altering the additives, facilitating a unified entry to diverse prenylated and reverse-prenylated oxindoles was available with varied nucleo- and electrophilic substitution.

2. Experimental

2.1. General information

^{1}H nuclear magnetic resonance (NMR) and ^{13}C NMR and ^{19}F NMR spectra were collected at room temperature in $CDCl_3$ on 400 or 700 MHz instrument. Flash column chromatography was performed on silica gel (200–300 mesh). Substrates **1** were synthesized according to the literature procedures. Isoprene, nickel catalyst and phosphine ligands were commercially available.

2.2. General experimental procedure for reverse-prenylated oxindoles *3*

In a glove-box, $Ni(cod)_2$ (0.02 mmol, 5.6 mg), PCy_3 (0.04 mmol, 11.2 mg) and freshly distilled THF (2.0 mL) were added in 4 mL pressure tube. The catalyst system was pre-stirred at room temperature for 15 min. Then oxindole **1** (0.20 mmol), Cs_2CO_3 (0.20 mmol, 75.2 mg) and isoprene **2a** (0.40 mmol, 40 μL) were added and tighten the cap. The resulting solution was further stirred at 60–100 °C for 24 h. Upon completion, the mixture was concentrated in vacuo and purified by silica chromatography with petroleum ether/EtOAc to afford the reverse-prenylated products **3**.

2.3. General experimental procedure for consecutive alkylation

The reverse-prenylated oxindole **3a** (0.10 mmol, 21.5 mg), NaH (60% dispersed in mineral oil, 0.12 mmol, 4.8 mg) and anhydrous DMF (0.5 mL) were added in 5 mL Schlenk tube under nitrogen atmosphere. Then electrophile (R*X*, *X* = Br or I, 0.20 mmol) were added to the solution at 0 °C and tighten the cap. The resulting mixture was further stirred at room temperature for 12 h. Upon completion, the mixture was extracted with ethyl acetate (5 × 10 mL) and the combined organic extracts were dried over Na_2SO_4. Next, the solution was filtered and concentrated in vacuo. Purification by silica chromatography with petroleum ether/EtOAc afforded the reverse-prenylated 3,3-disubstituted oxindoles **12**.

2.4. General experimental procedure for α-hydroxy-reverse-prenylated oxindoles *13*

The reverse-prenyl oxindole **3a** (0.15 mmol), Cs_2CO_3 (0.03 mmol, 9.8 mg), PPh_3 (0.30 mmol, 78.7 mg) and DMSO (0.5 mL) were added in oven dried 4 mL bottle. Next, the resulting solution was stirred vigorously under air and ambient temperature for 12 h. Upon completion, the mixture was extracted with ethyl acetate (5 × 3 mL). Then the organic phase was concentrated in vacuo and purified by silica chromatography with petroleum ether/EtOAc to afford the α-hydroxy-reverse-prenylated oxindoles **13**.

2.5. General experimental procedure for α-hydroxy-reverse-prenylated oxindoles *14*

The reverse-prenyl oxindole **3a** (0.15 mmol), NaH (60% dispersed in mineral oil, 1.5 equiv., 9.0 mg) and dry DMF (0.5 mL) were added in oven dried 4 mL bottle. Next, the resulting solution was stirred vigorously under air and ambient temperature for 12 h. Upon completion, the mixture was extracted with ethyl acetate (5 × 3 mL). Then the organic phase was concentrated in vacuo and purified by silica chromatography with petroleum ether-EtOAc to afford the α-hydroxy-prenylated oxindoles **14**.

2.6. General experimental procedure for prenylated dimeric oxindoles and spiro-oxindoles

The acetate protected prenylated alcohol **14a'** (0.10 mmol, 27.4 mg), nucleophilic reagent (Ar-H) (0.15 mmol), $In(OTf)_3$ (10 mol%, 5.6 mg) and dry DCE (0.5 mL) were added in 4 mL bottle. Next, the resulting solution was stirred at 60 °C for 12 h. The reaction was monitored by TLC and upon completion, the mixture was purified by silica chromatography with petroleum ether/EtOAc to afford the prenylated dimeric oxindoles and spiro-oxindoles **17**.

3. Results and discussion

3.1. Optimization for nickel catalyzed reverse-prenylation of oxindole with isoprene

Initially, *N*-methyl-2-oxindole (**1a**) and isoprene (**2a**) were used as the model substrates to test our hypothesis under earth abundant Ni catalysis (Table 1). When reaction was first performed in THF at 60 °C with bis(dicyclohexylphosphino)methane (dcpm) as the ligand, reverse-prenylated oxindole **3a** could be produced in 39% yield, accompanied by a complex mixture of regioisomers (**4a**–**6a**) and dual C3-functionalized side-products (**7a**–**9a**). While the assessment of the other bidentate phosphine ligands failed to improve the regio- and chemoselectivities (entries 2–4), it was pleased to find the formation of side-products **7a**–**9a** were drastically inhibited using NHC ligands (entries 5, 6). However, the regioselectivity still remained at low level (**3a** *vs.* **6a**) and a large scale of isoprene dimers were detected by GC-MS as well. Therefore, our attentions were shifted to investigate the monodentate phosphine ligands (entries 7–14). To our delight, **3a** could be obtained in 35% yield with acceptable regioselectivity when PPh_3 was used as ligand (entry 7). This encouraged us to further examine oth-

Table 1
Optimization for nickel catalyzed reverse-prenylation of oxindole with isoprene.

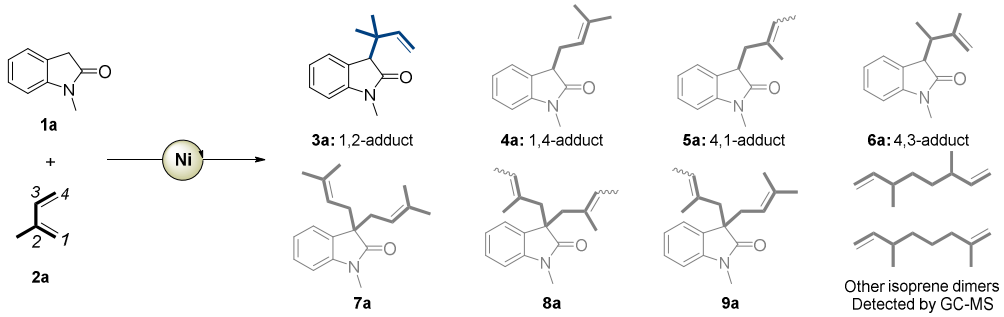

Entry	Ligand	Yield (%)					Entry	Ligand	Yield (%)				
		3a	**4a**	**5a**	**6a**	**(7a + 8a + 9a)** [c]			**3a**	**4a**	**5a**	**6a**	**(7a + 8a + 9a)** [c]
1	dcpm	39	2	1	12	42	8	PPh_2Cy	55	—	—	4	—
2	dcpe	1	1	2	9	85	9	$PPhCy_2$	77	—	—	5	—
3	dcpp	3	—	3	19	74	10	PCy_3	84	—	—	4	—
4	dcpb	14	—	19	30	28	11 [b]	PCy_3	96	—	—	2	—
5 [a]	IPr·HCl	77	—	—	10	—	12	CyJohnPhos	16	—	—	—	—
6 [a]	SIPr·HCl	56	—	—	20	—	13	SPhos	20	—	—	—	—
7	PPh_3	35	—	—	2	—	14	P^tBu_3	—	—	—	—	—

Conditions: **1a** (0.10 mmol), **2a** (0.20 mmol), $Ni(cod)_2$ (10 mol%), ligand (10 mol% for entries 1–6 or 20 mol% for entries 7–14), THF (1.0 mL), 60 °C, 12-24 h. Yields were determined by GC-FID analysis of the crude product mixture using mesitylene as internal standard. [a]MeONa (10 mol%). [b]Cs_2CO_3 (100 mol%). [c]The products (**7a**, **8a** and **9a**) were inseparable.

er analogous ligands. It was observed that the yield of **3a** could be steadily increased as the electron-rich ligands loaded, and PCy_3 was selected as the optimal choice where product **3a** could be furnished in 84% yield (entries 8–10). Notably, the addition of Cs_2CO_3 continued to improve the yield of reverse-prenylated product **3a** to 96% yield with maintained regio- and chemoselectivity (entry 11). Other common commercial ligands with bulky substituents, such as CyJohnPhos, SPhos and P^tBu_3 were all demonstrated to be harmful to the reaction outputs (entries 12–14).

3.2. Substrate scope of reverse-prenylated oxindoles and contiguous quaternary substituted oxindoles

With the optimized conditions in hand, the substrate scope for this Ni-catalyzed reverse-prenylation of oxindoles with isoprene was then evaluated (Fig. 2(A)). Subjecting *N*-methyl-2-oxindole (**1a**) to the standard conditions furnished reverse-prenylated oxindole **3a** in 94% isolated yield. Reverse-prenylation of oxindoles with different substituents (Et, Ph, Bn) on the nitrogen atom all proceeded smoothly to yield corresponding products **3b–3d**. In addition, substrates bearing *N*-allyl or *N*-isopentenyl group also showed good performance and delivered reverse-prenylated products **3e** or **3f** in good yields. Next, oxindoles with substituents on the benzene ring were investigated. Substrates with electron-donating groups, such as $-CH_3$ and $-OCH_3$, whether at the 5, 6 or 7-position, all afforded desirable products efficiently (**3g**, **3l**, **3n** and **3r**). Oxindoles with electron-withdrawing groups ($-CF_3$, halides and $-CO_2Me$) also could generate reverse-prenylated oxindoles in 70%-86% yields (**3h–3k**, **3m**, **3o–3q**). Moreover, the reaction still worked when the pyrrolo[2,3-*b*]pyridin-2-one was adopted as substrate and gave **3s** in 65% yield. Compared with isoprene (**2a**), 2,3-dimethylbutadiene (**2b**) is less reactive due to steric hindrance. Therefore, higher temperature (140 °C) was required to deliver corresponding products **10a–10d** in decent yields, though the impaired reactivity of product **10b** may be attributed to the steric hindrance of 5-methyl group on oxindole scaffold. Linalyl group is an important C10 skeleton among monoterpenoids. Therefore, myrcene **2c** was then subjected to this atom-economic protocol. Delightfully, the hydrofunctionalization of oxindoles with myrcene **2c** could successfully give C3-linalylated oxindoles (**11a–11d**) in moderate to good yields. Considering the electron-donating attribute of 6-methoxy groups, the decreased yield for **11b** may be attributed to the diminished nucleophilicity at C3-position of oxindoles, while the regioselectivity was significantly reduced under higher reaction temperature.

Utilizing the obtained reverse-prenylated products as nucleophiles, a consecutive alkylation with various alkyl halides was conducted to furnish contiguous quaternary substituted carbons (Fig. 2(B)) [33]. Under basic condition, nucleophilic substitution reactions with benzyl bromides generally offered the products **12a–12d** in excellent yields. Prenylation and geranylation also occurred efficiently at the pseudobenzylic position, affording corresponding products in 86% and 95% yields (**12e** and **12f**), respectively. Versatile synthetic blocks such as propargyl and cyano groups could be installed at the C3-position as well (**12g** and **12h**). While nucleophilic alkylation reactions with methyl or ethyl halides proceeded smoothly (**12i** and **12j**), the *O*-alkylated product was also observed due to steric hindrance when bulky isopropyl bromide was adopted

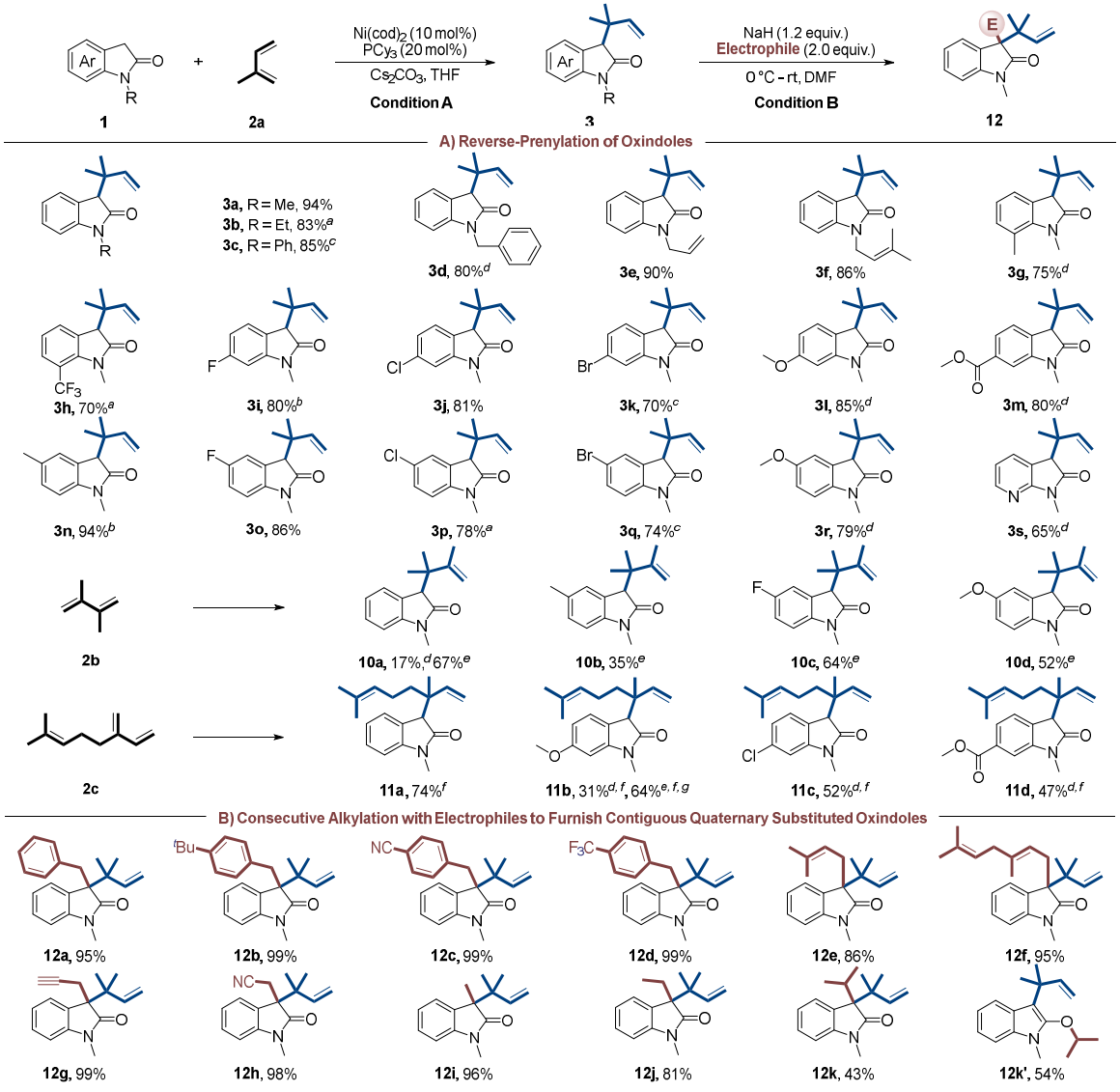

Condition A: **1** (0.20 mmol), **2** (0.40 mmol), Ni(cod)$_2$ (10 mol%), PCy$_3$ (20 mol%), Cs$_2$CO$_3$ (1.0 equiv.), THF (2.0 mL), N$_2$ atmosphere, 60 °C, 24 h. [a]70 °C. [b]80 °C. [c]90 °C. [d]100 °C. [e]1,4-dioxane (2.0 mL), 140 °C. [f]Dr = 2:1. [g]rr=72:28. Condition B: **3a** (0.10 mmol), NaH (1.2 equiv.), electrophile (RX, X = I or Br, 2.0 equiv.), DMF (0.50 mL), N$_2$ atmosphere, 0 °C – rt, 12 h.

Fig. 2. Substrate scope of reverse-prenylated oxindoles and contiguous quaternary substituted oxindoles.

(**12k** *vs.* **12k'**).

3.3. Substrate scope of α-hydroxy-(reverse-)prenylated oxindoles and consecutive (hetero)arylated oxindoles

3-Hydroxy-3-prenyl-oxindoles are often employed as key precursors in the synthesis of natural products and bioactive molecules [34]. However, established methods for the synthesis of this class of compounds mainly relied on pre-activated oxindoles (e.g. isatin or 3-hydroxy-2-oxindoles) [35,36]. Using air as green oxidant and PPh$_3$ as reductant, the α-hydroxylation of reverse-prenylated oxindoles was then investigated (Fig. 3(A)), which provided an efficient access to 3-hydroxy-3-reverse-prenylated oxindole **13a** in 98% yield. In this regard, not only *N*-prenyl substituted reverse-prenylated oxindole **13b** was obtained in good results, but also aromatic ring bearing methoxy group and halogen atoms showed high efficiency and gave products with up to 94% yield (**13c–13e**). To our surprise, with NaH as additive, the aerobic oxidation of C–H bond and the rearrangement of reverse-prenyl group could occur simultaneously to give quantitative α-hydroxylated prenylated oxindole **14a** (Fig. 3(B)). The examination of substrate scope showed that this transformation exhibited good functional groups tolerance. *N*-Protecting groups, such as alkyl, phenyl, allyl or prenyl, all complied with this α-hydroxylation. Electron-donating or withdrawing substituents, no matter which positions they located, displayed no obvious influence on reaction efficiency. Besides reverse-prenylated oxindoles, substrates **10a** and **11a** also went through this oxidative rearrangement steadily, producing corresponding products **15** and **16** in 86% and 80% yield respectively. The structure of **14e** was further confirmed by single crystal X-ray crystallography (CCDC: 2351892). The stereo configuration of **16** was determined by two-dimensional nuclear magnetic resonance

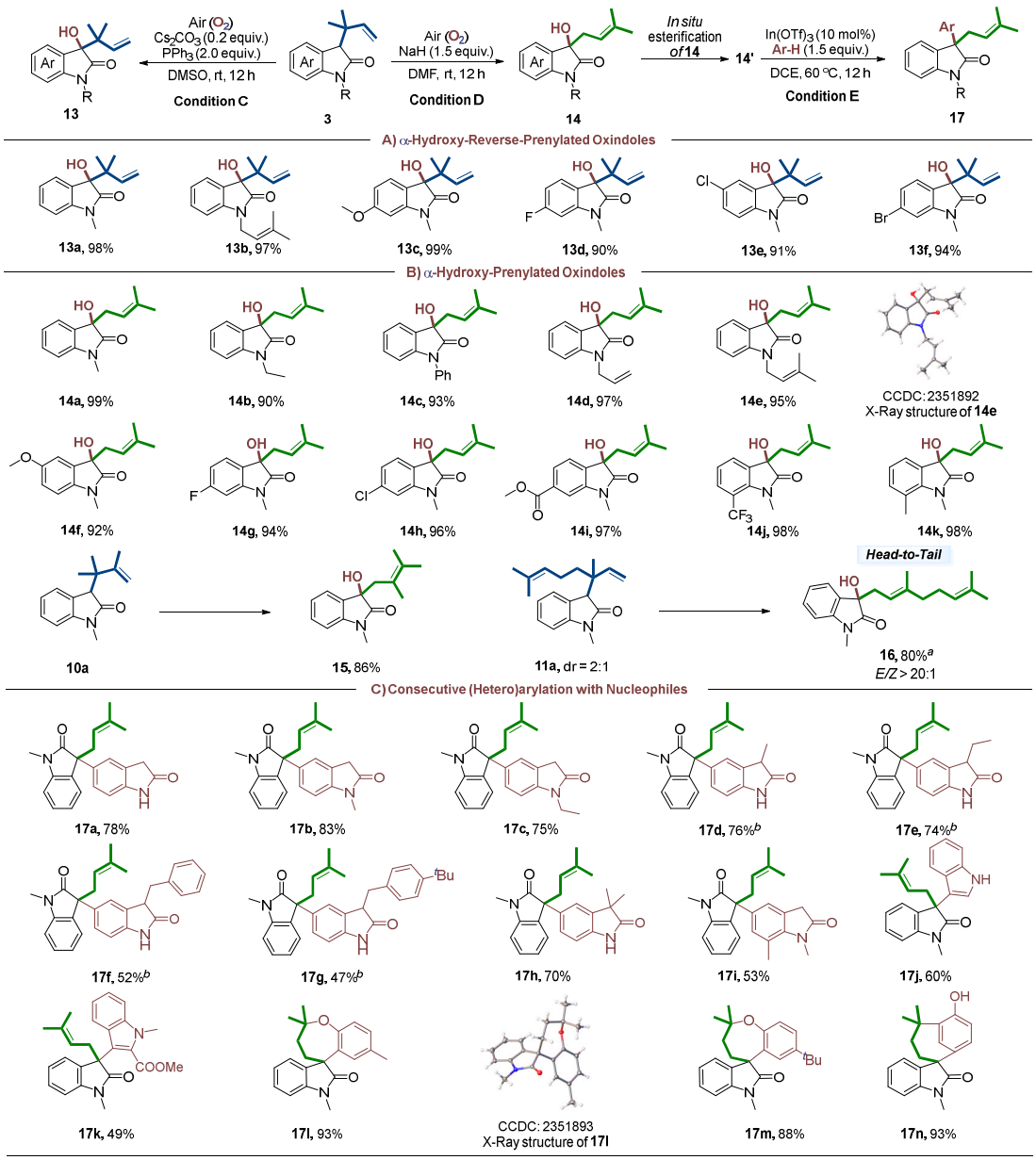

Condition C: **3** (0.15 mmol), Cs_2CO_3 (0.03 mmol), PPh_3 (0.30 mmol), DMSO (0.50 mL), under air, rt, 12 h. **Condition D:** **3** (0.15 mmol), NaH (1.5 equiv.), DMF (1.0 mL), under air, rt, 12 h. **Condition E:** **14'** (0.10 mmol), $In(OTf)_3$ (10 mol%), **Ar-H** (0.15 mmol), DCE (0.5 mL), 60 °C, 12 h. [a]40 °C, 24 h. [b]Dr = 1:1.

Fig. 3. Substrate scope of α-hydroxy-(reverse-)prenylated oxindoles and consecutive (hetero)arylated oxindoles.

(NOESY) spectroscopy.

The dimerization of indole skeletons is an important biosynthetic process to construct related alkaloids [37]. In this regard, the 3-hydroxy-3-prenylated oxindole **14a** could be converted into a useful synthon for oxindole dimerization after simple esterification (Fig. 3(C)). Employing Lewis acid $In(OTf)_3$ as catalyst, oxindoles could act as carbon nucleophiles to proceed Fridel-Crafts type transformation [38,39] with excellent C5-electivity whether bearing *N*-protecting groups or not (**17a–17c**). Substrates with naked or substituted C3-position also showed no obvious decrease in terms of regioselectivity (**17d–17i**). As for indoles, the nucleophilic substitution took place at C3-site, which gave **17j** and **17k** with good results. Interestingly, when subjecting *para*-substituted phenols as nucleophiles, an unexpected cascade annulation occurred to deliver oxa-spirocycles (**17l** and **17m**) in high yields. In contrast, when the reaction was performed with simple phenol, this cyclization reaction occurred exclusively between *ortho*- and *para*-position of phenol ring (**17n**). Notably, the structure of **17l** was confirmed by single crystal X-ray crystallography (CCDC: 2351893).

3.4. Mechanism studies for Ni-catalyzed reverse-prenylation of oxindoles with isoprene

According to our previous works and reported literatures, there were two distinct pathways mainly involved in mechanism for nickel-catalyzed hydrofunctionalization reactions:

Ni–H insertion [40–45] or ligand-to-ligand hydrogen transfer (LLHT) [46–53]. To gain insights into the mechanism, we performed a series of mechanistic experiments. Firstly, the interconversion reaction between oxindole **1b** and C3-deuterated oxindole **1a–1d** showed that hydrogen isotope exchange occurred at both benzylic sites of two substrates (Fig. 4(a)). For comparison, no deuterium incorporation was detected when reaction was performed in the absence of nickel and ligand (see supporting information for details: Table S4). The above results indicate that the nickel-hydride species may exist through oxidative addition step between oxindole and nickel(0) catalyst. This conclusion is also supported by the deuteration experiment, in which the C3-deuterated product **1a–1d** could be obtained by adding deuterium oxide to the oxindole-Ni(cod)$_2$-PCy$_3$ reaction mixture (Fig. 4(b)). It was found that deuterium scrambled into the gem-dimethyl groups, which

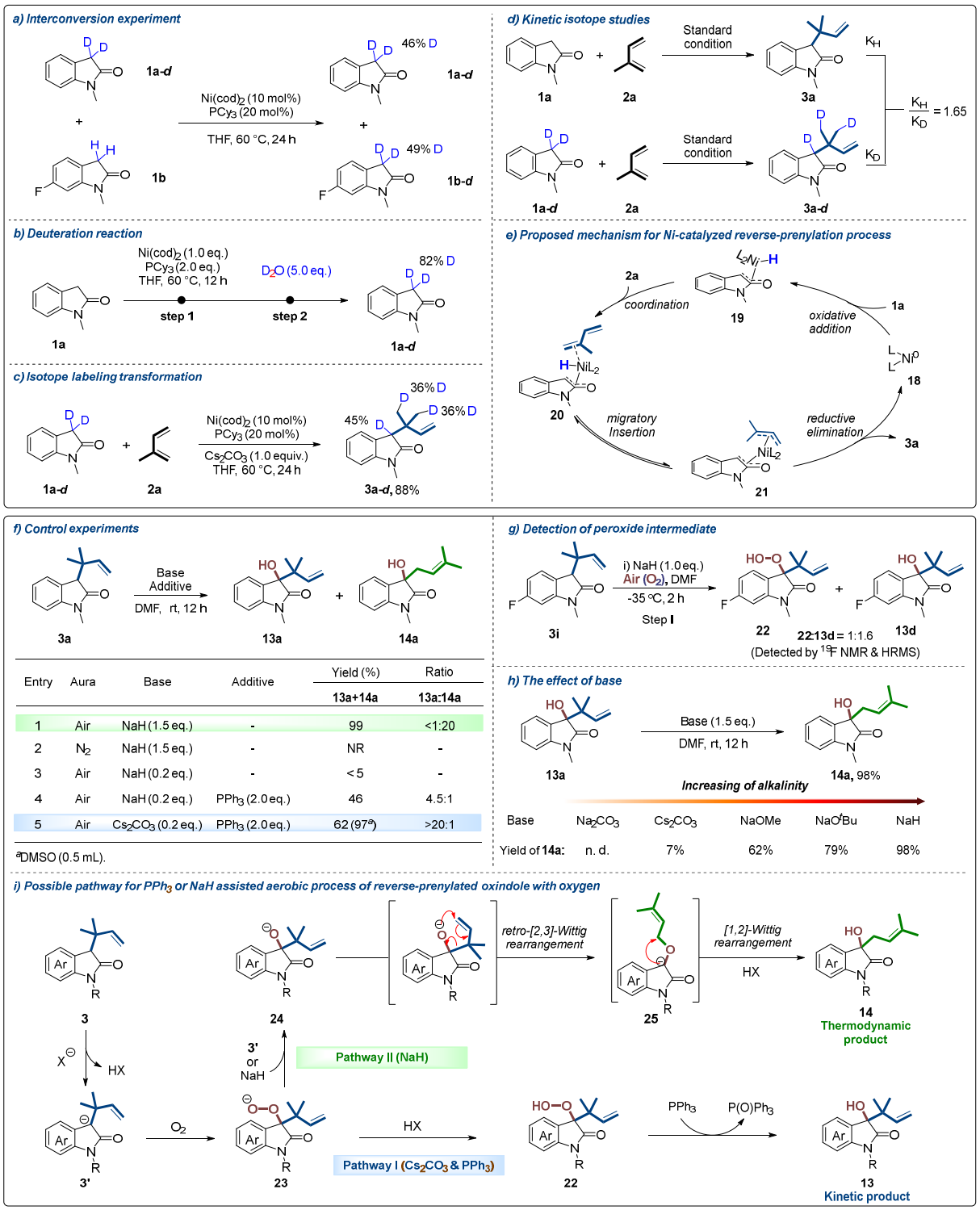

Fig. 4. Mechanism studies for unified construction of prenylated and reverse-prenylated oxindoles.

suggests a reversible step of Ni–H insertion in the catalytic cycle (Fig. 4(c)). Furthermore, a kinetic isotope effect (*KIE* = 1.65) is observed when reactions were performed with oxindole (**1a**) and deuterated oxindole (**1a–1d**) in parallel [54], supporting that either oxidative addition to the C–H bond or diene insertion into the Ni–H is the rate-determining step (Fig. 4(d)). Taking these studies into account, we propose the mechanism shown in Fig. 4(e). Initially, the oxidative addition of oxindole **1a** with nickel(0) species **18** gives the nickel-hydride intermediate **19**. Then the complex **19** coordinates isoprene **2a** to form desired Ni complex **20**. After reversible migratory insertion of alkene to Ni–H bond, the intermediate **21** is formed from complex **20**. Finally, the reductive elimination of intermediate **21** delivers reverse-prenylated product **3a** and regenerates nickel(0) species. Although we could not thoroughly exclude the LLHT mechanism, the Ni–H process seems more favorable based on current experimental results.

3.5. Mechanism studies of aerobic hydroxylation of reverse-prenylated oxindoles and prenyl-group rearrangement

To provide more information about the aerobic rearrangement reaction, several control experiments were conducted (Fig. 4(f)). First, no α-hydroxylated products could be detected when reaction operated in N_2 atmosphere, indicating the indispensable role of air (O_2) (entry 1 *vs.* 2). While reducing the loading amount of NaH to 0.2 equivalent resulted in little amount of corresponding product (entry 3), the 3-hydroxy-3-reverse-prenylated oxindole **13a** was unexpectedly obtained in majority when PPh_3 was added to the reaction system. According to literatures' report, the organophosphine reagent could accelerate the reduction of hydroperoxide (entry 4) [55–58]. Notably, replacing NaH with Cs_2CO_3 dramatically increased the yield to 62% (and 97% yield in DMSO) with excellent selectivity (>20:1) (entry 5). To probe the potential intermediates, α-hydroxylation reaction of **3i** was carried out at –35 °C with NaH as base (Fig. 4(g)). Fortunately, we observed a mixture of hydroperoxide **22** and hydroxylated product **13d** rather than prenyl-rearranged products.

These results encouraged us to directly convert 3-hydroxy-3-reverse-prenylated oxindole **13a** to prenyl-rearranged oxindole **14a**. As showed in the Fig. 4(h), no transformation of **13a** could be observed when weak base Na_2CO_3 was added into the reaction. However, the yield of oxindole **14a** was steadily raised along with the stronger bases employed [59]. It should also be noted that no crossed products were obtained when equal amount of reverse-prenylated indole **3i** and linalylated oxindole **11a** were subjected to oxidative rearrangement reactions, ruling out intermolecular rearrangement process (see supporting information for details). With above studies in hand, we speculated that α-hydroxylation reaction probably goes through the C–H oxidation first in the presence of air and base to yield peroxide anion intermediate **23** (Fig. 4(i)). In the presence of catalytic amount Cs_2CO_3, protonation of intermediate **23** gives hydroperoxide **22**, which will be reduced by PPh_3 to produce kinetic product **13** (Pathway I) [56]. On the other road, with excessive sodium hydride, intermediate **23** is reduced by oxindole anion **3'**[60] or sodium hydride to generate oxyanion **24**. The latter then proceeds through retro-[2,3]-Wittig rearrangement to furnish intermediate **25** [61]. Followed by *in situ* [1,2]-Wittig rearrangement [62,63], 3-hydroxy-3-prenyl-oxindoles **14** is eventually formed as a thermodynamic product (Pathway II).

3.6. Scale-up preparation and divergent transformations

To further demonstrate the synthetic potential, scale-up reactions along with consecutive derivatizations were performed. As depicted in Fig. 5(a), the nickel-catalyzed reverse-prenylation of oxindoles **1a**, **3i** and **3f** could be easily scaled up without any loss of efficiency. The skeletally divergent α-hydroxylation of reverse-prenylated oxindole **3f** was successfully conducted on a 1.0 mmol scale, giving 3-hydroxy-3-(reverse-)prenylated oxindoles **13b** and **14m** respectively. In the outset, divergent transformations were carried out with the obtained products (Fig. 5(b)). Interestingly, the Simmons-Smith type cyclopropanation of **13b** occurred exclusively at the terminal alkene with 97% yield under cobalt catalysis [64]. With Lewis acid $In(OTf)_3$ as catalyst, the tetrahydrofuran fused spirooxindole **29** was obtained in 87% yield via intramolecular electrophilic addition. In addition, Appel reaction of 3-hydroxy-3-prenyl-oxindole **14m** was carried out to deliver brominated product **26** in decent yield, which then reacted with malononitrile to give C3-disubstituted oxindole **30**. On the other hand, the prenylated oxindole **4b** bearing unsubstituted benzylic C–H bond could be steadily acquired by simple debromination 3-bromo-3-prenyl-oxindole **26** with $NaBH_4$. And a subsequent nucleophilic substitution with 2-bromoacetonitrile efficiently produced **31** on a 2.0 mmol scale. Similarly, the reaction of reverse-prenyloxindole **13f** with 2-bromoacetonitrile offered product **28** in 89% yield.

Taking advantage of the versatile reactivity of cyano group, further transformations of products **28** and **31** were investigated subsequently (Fig. 5(c)). In the presence of $LiAlH_4$, reduction and cyclization of oxindole **28** could be performed in one pot, giving bicyclic product **32** (a precursor of debromoflustramine A) in 72% yield. Such operation could also be applied for the synthesis of alkaloid **35**, which could be converted to debromoflustramine B after methylation [7]. Under alkaline condition, cyanide could be transformed into carboxyl group and gave carboxylic acid **33** in 96% yield. Following condensation, amide **34** was obtained in 90% yield. On the other side, reduction of **31** under elevated temperature directly offered indoline **36** in good yield [65], while the amidation process by the aid of H_2O_2 took place to deliver 90% yield of amide **37**.

4. Conclusions

In conclusion, we have developed a unified approach to access structurally divergent prenylated and reverse-prenylated oxindoles. Launched by reverse-prenylation of C3-unsubstituted oxindoles with isoprene, excellent regio- and chemo-selectivities were obtained under nickel catalysis. Taking advantage of the reserved benzylic C–H bonds in obtained

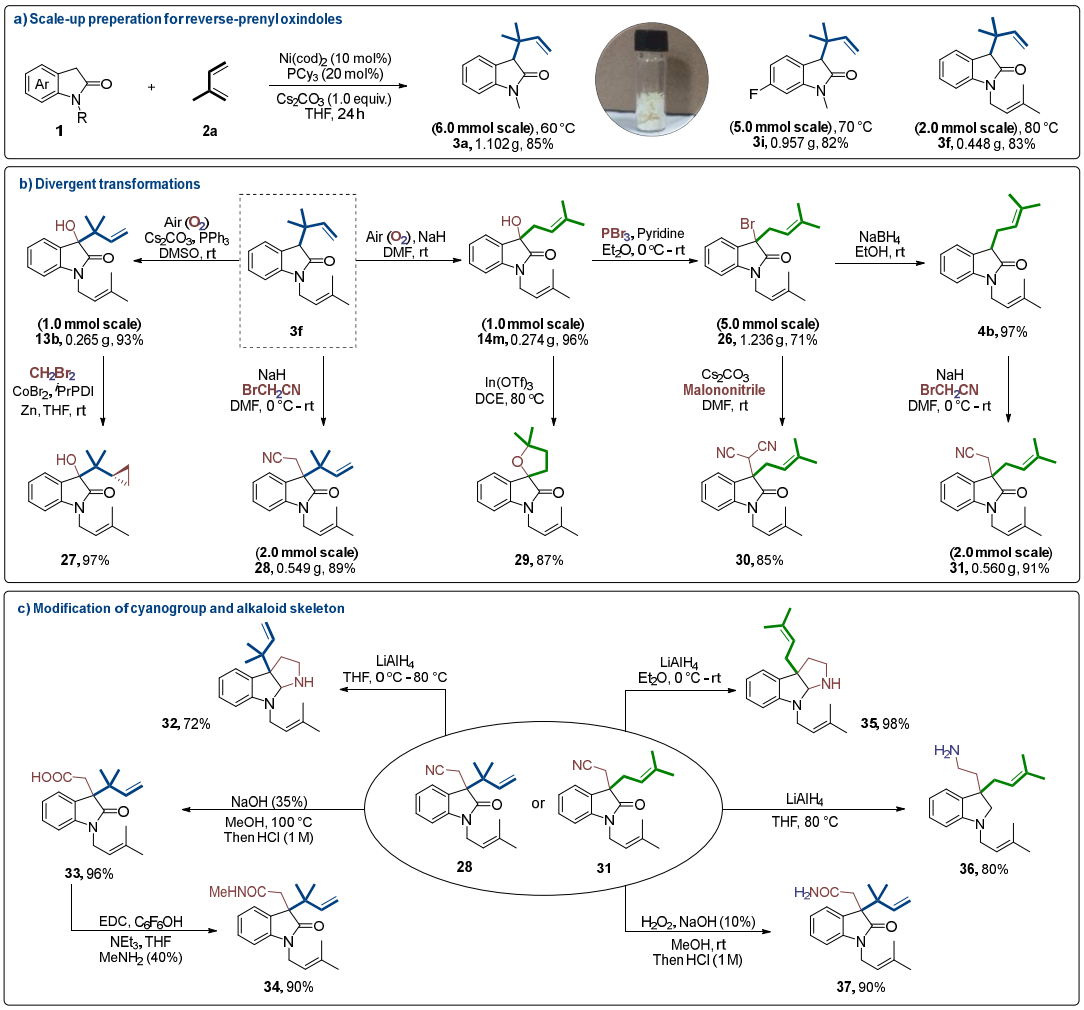

Fig. 5. Scale-up preparation and divergent transformations.

reverse-prenylated oxindoles, a series of alkylated functionalization were performed to create vicinal quaternary centers. With molecular oxygen as the oxidant, prenylated or reverse-prenylated α-hydroxy-oxindoles could also been achieved selectively by the choice of base and promoter (PPh_3). After *in situ* esterification, the Friedel-Crafts alkylation reactions took place with electron-rich aromatic nucleophiles to deliver prenyl-substituted dimeric oxindoles or spirooxindoles. Furthermore, various transformations of obtained products have been demonstrated to provide efficient access to bioactive intermediates.

Data Availability

Crystallographic data for the structures reported in this Article have been deposited at the Cambridge Crystallographic Data Centre, under deposition numbers CCDC: 2351892 (**14e**) and CCDC: 2351893 (**17i**). Copies of the data can be obtained free of charge *via* https://www.ccdc.cam.ac.uk/structures/. Data relating to the characterization data of materials and products, general methods, optimization studies, experimental procedures, mechanistic studies and NMR spectra are available in the Supplementary Information. All data are also available from the corresponding author upon request.

Electronic supporting information

Supporting information is available in the online version of this article.

References

[1] R. J. Melander, A. K. Basak, C. Melander, *Nat. Prod. Rep.*, **2020**, 37, 1454–1477.
[2] D. Crich, A. Banerjee, *Acc. Chem. Res.*, **2007**, 40, 151–161.
[3] E. Oldfield, F. Y. Lin, *Angew. Chem. Int. Ed.*, **2012**, 51, 1124–1137.
[4] C. Marti, E. M. Carreira, *J. Am. Chem. Soc.*, **2005**, 127, 11505–11515.
[5] A. W. Grubbs, G. D. Artman, S. Tsukamoto, R. M. Williams, *Angew. Chem. Int. Ed.*, **2007**, 46, 2257–2261.
[6] T. Kawasaki, M. Shinada, M. Ohzono, A. Ogawa, R. Terashima, M. Sakamoto, *J. Org. Chem.*, **2008**, 73, 5959–5964.
[7] T. Kawasaki, A. Ogawa, R. Terashima, T. Saheki, N. Ban, H. Sekiguchi, K. E. Sakaguchi, M. Sakamoto, *J. Org. Chem.*, **2005**, 70, 2957–2966.
[8] R. Craig, E. Sorrentino, S. J. Connon, *Chem. Eur. J.*, **2018**, *24*, 4528–4531.

Graphical Abstract

Chin. J. Catal., 2025, 70: 444–454 doi: 10.1016/S1872-2067(24)60218-4

Unified construction of prenylated and reverse-prenylated oxindoles from isoprene launched by Ni catalysis

Ying-Ying Liu, Ying Li, Xue-Ting Li, Su-Yang Xu, Ding-Wei Ji *, Xiang-Ping Hu *, Qing-An Chen *
Dalian Institute of Chemical Physics, Chinese Academy of Sciences; University of Chinese Academy of Sciences

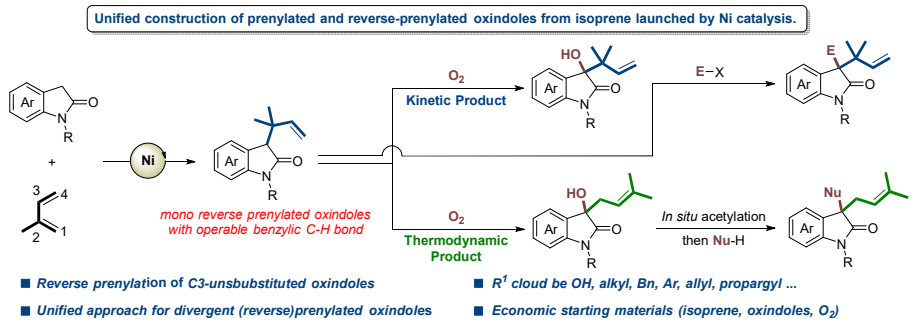

A unified approach has been developed to access structurally divergent prenylated and reverse-prenylated oxindoles. Launched by nickel-catalyzed reverse-prenylation of C3-unsubstituted oxindoles with isoprene, hydroxylation or substitutions at the pseudobenzylic position with various functional groups created vicinal quaternary centers in a concise way.

[9] X. Zuo, Z. H. Wan, Z. H. Liao, C. Wang, C. H. Tan, S. D. Huo, L. L. Zong, *ACS Catal.,* **2023**, 13, 15708–15714.
[10] L. M. Zhao, A. L. Zhang, J. H. Zhang, H. S. Gao, W. Zhou, *J. Org. Chem.,* **2016**, 81, 5487–5494.
[11] B. Alcaide, P. Almendros, R. Rodríguez-Acebes, *J. Org. Chem.,* **2005**, 70, 3198–3204.
[12] Y. Hou, J. Y. Huo, R. X. Li, J. Hou, P. Lei, H. B. Wei, W. Q. Xie, *Org. Lett.,* **2023**, 25, 6949–6953.
[13] T. Kawasaki, M. Shinada, D. Kamimura, M. Ohzono, A. Ogawa, *Chem. Commun.,* **2006**, 420–422.
[14] K. Thandavamurthy, D. Sharma, S. K. Porwal, D. Ray, R. Viswanathan, *J. Org. Chem.,* **2014**, 79, 10049–10067.
[15] V. Ignatenko, N. Deligonul, R. Viswanathan, *Org. Lett.,* **2010**, 12, 3594–3597.
[16] T. Kawasaki, M. Nagaoka, T. Satoh, A. Okamoto, R. Ukon, A. Ogawa, *Tetrahedron,* **2004**, 60, 3493–3503.
[17] T. Kawasaki, R. Terashima, K. E. Sakaguchi, H. Sekiguchi, M. Sakamoto, *Tetrahedron Lett.,* **1996**, 37, 7525–7528.
[18] X. X. Chang, F. Q. Zhang, S. B. Zhu, Z. Yang, X. M. Feng, Y. B. Liu, *Nat. Commun.,* **2023**, 14, 3876.
[19] Y. C. Hu, X. T. Min, D. W. Ji, Q. A. Chen, *Trends Chem.,* **2022**, 4, 658–675.
[20] L. Susse, B. M. Stoltz, *Chem. Rev.,* **2021**, 121, 4084–4099.
[21] P. S. Wang, L. Z. Gong, *Acc. Chem. Res.,* **2020**, 53, 2841–2854.
[22] Q. Cheng, H. F. Tu, C. Zheng, J. P. Qu, G. Helmchen, S. L. You, *Chem. Rev.,* **2019**, 119, 1855–1969.
[23] B. M. Trost, M. L. Crawley, *Chem. Rev.,* **2003**, 103, 2921–2943.
[24] B. M. Trost, D. L. V. Vranken, *Chem. Rev.,* **1996**, 96, 395–422.
[25] B. M. Trost, S. Malhotra, W. H. Chan, *J. Am. Chem. Soc.,* **2011**, 133, 7328–7331.
[26] T. Y. Chen, M. J. Krische, *Org. Lett.,* **2013**, 15, 2994–2997.
[27] C. Y. Zhao, Y. Y. Liu, X. X. Zhang, G. C. He, H. Liu, D. W. Ji, Y. C. Hu, Q. A. Chen, *Angew. Chem. Int. Ed.,* **2022**, 61, e202207202.
[28] G. Zhang, C. Y. Zhao, X. T. Min, Y. Li, X. X. Zhang, H. Liu, D. W. Ji, Y. C. Hu, Q. A. Chen, *Nat. Catal.,* **2022**, 5, 708–715.
[29] W. S. Jiang, D. W. Ji, W. S. Zhang, G. Zhang, X. T. Min, Y. C. Hu, X. L. Jiang, Q. A. Chen, *Angew. Chem. Int. Ed.,* **2021**, 60, 8321–8328.
[30] C. S. Kuai, D. W. Ji, C. Y. Zhao, H. Liu, Y. C. Hu, Q. A. Chen, *Angew. Chem. Int. Ed.,* **2020**, 59, 19115–19120.
[31] Y. C. Hu, D. W. Ji, C. Y. Zhao, H. Zheng, Q. A. Chen, *Angew. Chem. Int. Ed.,* **2019**, 58, 5438–5442.
[32] G. Zhang, W. S. Zhang, X. Y. Wang, Y. Yang, D. W. Ji, B. S. Wan, Q. A. Chen, *Chin. J. Catal.,* **2023**, 49, 123–131.
[33] C. D. Grant, M. J. Krische, *Org. Lett.,* **2009**, 11, 4485–4487.
[34] J. H. Zhang, R. B. Wang, D. F. Li, L. M. Zhao, *ACS Omega,* **2017**, 2, 7022–7028.
[35] M. Retini, G. Bergonzini, P. Melchiorre, *Chem. Commun.,* **2012**, 48, 3336–3338.
[36] M. Silvi, I. Chatterjee, Y. K. Liu, P. Melchiorre, *Angew. Chem. Int. Ed.,* **2013**, 52, 10780–10783.
[37] H. Takayama, I. Mori, M. Kitajima, N. Aimi, N. H. Lajis, *Org. Lett.,* **2004**, 6, 2945–2948.
[38] K. N. Babu, L. K. Kinthada, S. Ghosh, A. Bisai, *Org. Biomol. Chem.,* **2015**, 13, 10641–10655.
[39] L. K. Kinthada, S. Ghosh, K. N. Babu, M. Sharique, S. Biswas, A. Bisai, *Org. Biomol. Chem.,* **2014**, 12, 8152–8173.
[40] N. A. Eberhardt, H. Guan, *Chem. Rev.,* **2016**, 116, 8373–8426.
[41] A. J. Nett, J. Montgomery, P. M. Zimmerman, *ACS Catal.,* **2017**, 7, 7352–7362.
[42] L. J. Xiao, L. Cheng, W. M. Feng, M. L. Li, J. H. Xie, Q. L. Zhou, *Angew. Chem. Int. Ed.,* **2017**, 57, 461–464.
[43] Y. G. Chen, B. Shuai, X. T. Xu, Y. Q. Li, Q. L. Yang, H. Qiu, K. Zhang, P. Fang, T. S. Mei, *J. Am. Chem. Soc.,* **2019**, 141, 3395–3399.
[44] X. Y. Lv, C. Fan, L. J. Xiao, J. H. Xie, Q. L. Zhou, *CCS Chem.,* **2019**, 1, 328–334.
[45] J. Long, Y. Q. Li, W. N. Zhao, G. Y. Yin, *Chem. Sci.,* **2022**, 13, 1390–1397.
[46] J. Guihaumé, S. Halbert, O. Eisenstein, R. N. Perutz, *Organometallics,* **2011**, 31, 1300–1314.
[47] S. Tang, O. Eisenstein, Y. Nakao, S. Sakaki, *Organometallics,* **2017**, 36, 2761–2771.
[48] L. Cheng, M. M. Li, L. J. Xiao, J. H. Xie, Q. L. Zhou, *J. Am. Chem. Soc.,* **2018**, 140, 11627–11630.

[49] J. S. Marcum, T. R. Taylor, S. J. Meek, *Angew. Chem. Int. Ed.,* **2020**, 59, 14070–14075.
[50] L. Cheng, M. M. Li, M. L. Li, L. J. Xiao, J. H. Xie, Q. L. Zhou, *CCS Chem.,* **2022**, 4, 2612–2619.
[51] J. F. Li, D. Pan, H. R. Wang, T. Zhang, Y. Li, G. P. Huang, M. C. Ye, *J. Am. Chem. Soc.,* **2022**, 144, 18810–18816.
[52] Q. Li, Z. Wang, V. M. Dong, X. H. Yang, *J. Am. Chem. Soc.,* **2023**, 145, 3909–3914.
[53] Z. H. Chen, L. J. Gu, B. Wang, L. J. Xiao, M. C. Ye, Q. L. Zhou, *J. Am. Chem. Soc.,* **2024**, 146, 14915–14921.
[54] X. H. Yang, R. T. Davison, S. Z. Nie, F. A. Cruz, T. M. McGinnis, V. M. Dong, *J. Am. Chem. Soc.,* **2019**, 141, 3006–3013.
[55] D. Sano, K. Nagata, T. Itoh, *Org. Lett.,* **2008**, 10, 1593–1595.
[56] Y. F. Liang, N. Jiao, *Angew. Chem. Int. Ed.,* **2014**, 53, 548–552.
[57] S. B. D. Sim, M. Wang, Y. Zhao, *ACS Catal.,* **2015**, 5, 3609–3612.
[58] C. Xu, X. Li, L. Bai, *J. Org. Chem.,* **2022**, 87, 4298–4304.
[59] E. J. Bailey, D. H. R. Barton, J. Elks, J. F. Templeton, *J. Chem. Soc.,* **1962**, 1578–1591.
[60] M. B. Chaudhari, Y. Sutar, S. Malpathak, A. Hazra, B. Gnanaprakasam, *Org. Lett.,* **2017**, 19, 3628–3631.
[61] M. Tsubuki, H. Okita, T. Honda, *J. Chem. Soc., Chem. Commun.,* **1995**, 2135–2136.
[62] Y. Katsuyama, X. W. Li, R. Müller, B. Nay, *ChemBioChem.,* **2014**, 15, 2349–2352.
[63] D. Mal, K. Ghosh, S. Jana, *Org. Lett.,* **2015**, 17, 5800–5803.
[64] J. Werth, C. Uyeda, *Chem. Sci.,* **2018**, 9, 1604–1609.
[65] M. H. Sun, L. S. Wei, C. K. Li, *J. Am. Chem. Soc.,* **2023**, 145, 3897–3902.

镍催化吲哚酮的选择性异戊烯化和反异戊烯基化反应

刘盈盈[a,b], 李　莹[a,b], 李雪婷[a,b], 徐溯阳[a,b], 季定纬[a,*], 胡向平[a,b,*], 陈庆安[a,b,*]
[a]中国科学院大连化学物理研究所, 辽宁大连116023
[b]中国科学院大学, 北京100049

摘要: C3戊烯基或反异戊烯基取代的吲哚酮是许多具有重要生物活性的天然产物和药物分子的骨架结构, 因此开发吲哚酮的高效异戊烯基或反异戊烯基化方法吸引了有机和药物化学家的广泛关注. 传统上, 在过量碱的存在下通过吲哚酮与异戊烯基卤代物的亲核取代反应, 可以实现吲哚酮的C3异戊烯基化反应. 但这类反应往往缺乏原子经济性且反应的选择性主要依赖于底物结构性质. 利用过渡金属催化体系, 则可以实现对反应选择性的有效调控. 但文献中已报道的反应方法均需要在吲哚酮的C3位置预先引入一个取代基, 这限制了产物后续的转化利用. 目前为止, 对于C3未取代吲哚酮的选择性异戊烯基或反异戊烯基化反应依然是一项挑战性的工作.

基于前期关于异戊二烯氢官能团化反应的研究, 本文使用丰产金属镍与单齿膦配体的催化体系, 以较好的化学和区域选择性实现了C3未取代吲哚酮与异戊二烯的反异戊烯基化反应. 机理上反应首先经历零价镍与吲哚酮C–H键的氧化加成, 生成二价镍-氢金属物种, 随后该物种再与异戊二烯配位以及迁移插入, 最后通过还原消除获得目标产物. 该反应过程中没有当量副产物生成, 具有原子经济性. 利用吲哚酮产物在C3位还有一个活泼反应位点的优势, 可以通过一系列亲核取代反应快速构建结构多样性的3,3-二取代吲哚酮. 此外, 利用对反应添加剂(碱, 三苯基膦)的调控, 在空气氛围中实现了反异戊烯基取代吲哚酮产物的C–H选择性羟基化反应, 发散性地得到反异戊烯基和戊烯基取代的α-羟基-吲哚酮. 机理研究表明, 在碳酸铯/三苯基膦反应体系中, 反异戊烯基取代吲哚酮C3位点的C-H键被碱活化, 并被空气中的氧气氧化生成过氧化物, 最后在三苯基膦的还原作用下生成C3-羟基化的动力学产物. 而在过量的氢化钠强碱体系中, C3位点上的反戊烯基先后进行的逆-[2,3]-Witting重排和[1,2]-Witting-重排, 最后生成热力学稳定的戊烯基取代的羟基化产物. 将该羟基化产物原位酯化后, 可以通过傅-克反应与吲哚酮C5位点偶联, 高效地构建二聚吲哚酮骨架; 或与苯酚反应得到结构新颖的螺环化合物. 最后, 基于吲哚酮骨架结构对产物进行了多样性转化, 并实现了天然产物debromoflustramine A和B前体的合成.

综上, 本文在金属镍催化条件下实现了C3未取代吲哚酮的选择性反异戊烯基化反应. 利用产物C3位的活泼C-H键, 可以通过亲核取代、C-H键选择性氧化羟基化, 以及随后的亲电取代或环化反应, 实现结构丰富的异戊烯基和反戊烯基取代吲哚酮产物的快速构建, 为相关生物碱天然产物和药物分子的合成与制备提供了新思路.

关键词: 镍催化; 一体化合成; 异戊二烯; (反)异戊烯基化; 吲哚酮

收稿日期: 2024-12-03. 接受日期: 2024-12-30. 上网时间: 2025-03-20.
*通讯联系人. 电子信箱: dingweiji@dicp.ac.cn (季定纬), xiangping@dicp.ac.cn (胡向平), qachen@dicp.ac.cn (陈庆安).
基金来源: 国家自然科学基金(22201281, 22071239, 22371275).